Korean J. Chem. Eng., 39(5), 1194-1206 (2022)
DOI: 10.1007/s11814-022-1077-4

pISSN: 0256-1115
eISSN: 1975-7220

Three-step short-time temperature-programmed hydrothermal synthesis of ZSM-5 with high durability for conversion of methanol to propylene

Parisa Sadeghpour*, and Mohammad Haghighi*,**,†**

*Chemical Engineering Faculty, Sahand University of Technology, P. O. Box 51335-1996, Sahand New Town, Tabriz, Iran
**Reactor and Catalysis Research Center (RCRC), Sahand University of Technology,
P. O. Box 51335-1996, Sahand New Town, Tabriz, Iran
(*Received 30 November 2017 • Revised 15 April 2018 • Accepted 30 April 2018*)

Abstract−Three-step high temperature programmed hydrothermal preparation of ZSM-5 was investigated by using different crystallization times and temperatures. The synthesized nanostructured catalysts were analyzed by XRD, FESEM, EDX, BET-BJH, FTIR, TPD-NH_3 and TGA techniques. According to the obtained characterization results, synthesis of ZSM-5(250-30,300-15,350-5) by short time temperature programmed showed a significant effect on the crystallinity, phase purity, morphology, textural properties and acidity of the nanostructured catalyst. Furthermore, this sample had small crystals with higher intercrystalline porosity and also proper distribution of acid sites. The synthesized catalysts were applied in the methanol to propylene (MTP) process under the operating conditions of T=460 °C and GHSV=10,500 cm^3/g_{cat}·h in a fixed-bed reactor. The ZSM-5(250-30,300-15,350-5) catalyst exhibited high selectivity toward propylene (73%) with slow deactivation rate. Also, the possible reaction pathway for pure MFI preparation via three-step short-time temperature-programmed was presented.

Keywords: ZSM-5, High Temperature, Short Time, Three-step, Methanol, Propylene

INTRODUCTION

Methanol transformation to more useful hydrocarbons is one of the most important topics of natural gas utilization. In an alternative process, methane is first transferred to synthesis gas by partial oxidation or reforming [1,2], followed by conversion to methanol employing a $Cu/ZnO/Al_2O_3$ catalyst [3] and then converted to hydrocarbons using the methanol to gasoline (MTG) [4,5], methanol to olefins (MTO) or methanol to propylene (MTP) pathways [6,7]. These provide an indirect route for creating valuable products by converting fossil fuels [2,8,9]. The MTO reaction is an innovative way for the production of olefins from natural gas [10-12]. It offers yield flexibility that can deliver propylene as well as ethylene and can be designed for an ethylene-to propylene ratio between 0.75 and 1.5 with ethylene formation favored at higher severity [13-15]. But, the future demand of propylene is much larger than that for ethylene, and this gap can probably only be bridged by application of the MTP reaction [16,17].

A highly siliceous ZSM-5 catalyst with a medium pore aluminosilicate framework is a zeolite that is employed as a catalyst in various processes [18,19]. It also represents a group of crystalline microporous aluminosilicates that has been employed as the acidic framework in the MTP reaction [20-22]. The efficiency of the MTP process has been improved through modifying the reaction condition, the catalyst structure and also the shape selectivity of the zeolite [11,17,23]. For a specific ZSM-5 molecular sieve, there are still spaces and challenges in using different synthesis conditions that affect the nature and physicochemical properties of molecular species, which dictate the final product distribution [24,25]. High-quality ZSM-5 zeolite can be synthesized via the hydrothermal method [22,26,27]. The characterization indicates that the hydrothermal synthesis mechanism of the MFI framework has three steps [28,29]. First, the formation of amorphous particles occurs by mixing the reactants. Second, the nuclei appear with aggregation of amorphous particles into larger units as secondary particles. Finally, the secondary particles convert to the ZSM-5 molecular sieve by zeolitization [6,24,30]. Therefore, ZSM-5 zeolite may be prepared from the initial reaction gel by strictly controlling the crystallization condition. Different crystallization conditions, like SiO_2/Al_2O_3 ratio in the gel mixture, the reaction materials, time and temperature of crystallization, can influence the structure, property, type and morphology of products [23,31]. In this manner, a certain time and appropriate temperature of crystallization lead to the formation of products. On the other hand, the dense phases can be synthesized without the appropriate ranges of temperature and time for crystallization. In the work done by Oleksiak and Rimer [32], increasing the crystallization time led to a change of mordenite framework inverted (MFI) structure to mordenite (MOR) due to the unstable nature of the MFI phase in this certain synthesis condition. Moreover, the high crystallization temperature resulted in the decreasing of crystallization time. In this regard, Dargahi and et al. [33] showed that when the crystallization temperature of SAPO-34 was increased from 468 to 673 K, the hydrothermal crystallization time was decreased from 24 h to 45 min.

The high temperature crystallization conditions can accelerate the dissolution of the nutrients with controlled size, shape, morphology

†To whom correspondence should be addressed.
E-mail: haghighi@sut.ac.ir
Copyright by The Korean Institute of Chemical Engineers.

of particles and the structure of which phase composition is obtained during the crystallization [34,35]. It also allows thte production of the proper topology of the MFI structure of ZSM-5 with a cost-effective and high-throughput procedure [24]. On the other hand, the hydrothermal method contains many simultaneous reactions that occur in an aqueous system to form specific materials. The hydrothermal synthesis of MFI frameworks with regular arrays of channels and voids architecture is emerging as the key due to their structural advantages [23,30,33]. To take advantage of the hydrothermal synthesis method, it is significant to choose a hydrothermal system that can be reactive and cost-effective. The reactivity of the hydrothermal approach can only be dependent on modifying the processing variables (such as reagent concentrations, temperature, pH, and pressure), which can be affected the crystallization process, as well as physicochemical properties of synthesized materials [11,24]. In this case, multi-step hydrothermal synthesis is a more suitable novel method, as specific structure design and corresponding controllable synthesis, which offers the possibility to fabricate for efficient use of energy [36]. The multi-step hydrothermal synthesis with a temperature program has the advantage of combining the one-step methods and creating an efficient route to the synthesis of zeolites [37-39]. Through step-by-step hydrothermal synthesis, the crystallization process frequently operates at different temperatures for different crystallization times. Along with the variation of crystallization temperature during hydrothermal synthesis, the concept of nucleation is modified. The multi-step hydrothermal synthesis has several advantages, such as an enhancement of crystallization rate, homogeneous nucleation, uniform morphology, specific pore geometry and rapid analog synthesis. On the other hand, compared to the single-step hydrothermal synthesis, the multi-step approach for ZSM-5 synthesis can control nucleation and crystal growth, which is favorable for the formation of particles with narrow size distribution [38]. Furthermore, the one-step hydrothermal method with long periods of crystallization time may increase energy consumption. The use of a multi-step temperature programmed hydrothermal synthetic method instead of conventional heating often results in good yields in a short time and decreases the consumption of energy, so contributes efficiently to the low cost of synthesis [36]. Wang et al. compared the performance of chabazite (CHA) structures of SAPO-34 prepared by conventional one-step hydrothermal crystallization and also a novel two-step varying-temperature hydrothermal crystallization syntheses [38]. They explained that the two-step hydrothermal treatment led to the largest surface area and allowed the fast diffusion of materials to the reaction media. However, compared with the amount of literature investigated about the single-hydrothermal synthesis of zeolites, little experimental evidence has been published on the multi-step hydrothermal synthesis method. Also, we have not been able to find any literature publications on multi-step high temperature programmed and short time hydrothermal synthesis of MFI molecular sieve used for olefins production.

The main goal of the present work was to investigate a novel three-step high temperature programmed hydrothermal crystallization to achieve the short synthesis time required for obtaining the pure ZSM-5 phase. For this purpose, three kinds of ZSM-5 materials were prepared with various crystallization times at any high temperature (250, 300 and 350 °C) programmed for hydrothermal preparation. The samples were analyzed by X-ray diffraction (XRD), field emission scanning electron microscopy (FESEM), energy dispersive X-ray (EDX), Brunner, Emmett and Teller-Barrett, Joyner and Halenda (BET-BJH), Fourier transform infrared (FTIR), temperature-programmed desorption of ammonia (TPD-NH_3) and thermo-gravimetric analysis (TGA) techniques. Finally, the catalytic performance of synthesized zeolites in the MTP process was also tested.

EXPERIMENTAL

1. Chemicals

ZSM-5 catalysts were synthesized by a three-step short time temperature programmed hydrothermal method with tetra-propylammonium bromide (TPABr, 99.9%, Merck) as a structure-directing agent. Sodium hydroxide (NaOH, 97%, Merck), sodium aluminate ($NaAlO_2$, 99%, Riedel-deltane Haën) and fumid silica (SiO_2, 99.8%, Aldrich) were employed as Na, Al and Si sources, respectively. Ammonium nitrate (NH_4NO_3, 99%, Merck) and deionized water (Kasra Company) were also used as an ion-exchanged aqueous solution and synthesis medium, respectively.

2. Preparation of Materials

A Three-step hydrothermal procedure with different crystallization times was used for the synthesis of ZSM-5 catalysts. The syn-

Table 1. Structural properties of three step high temperature short time synthesis of ZSM-5

Catalyst	Temperature programmed steps (T°C-Duration min)			Impurity phase	S_{BET} $(m^2/g)^a$	V_{Total} $(cm^3/g)^b$	V_{Micro} $(cm^3/g)^c$	V_{Meso} $(cm^3/g)^d$	Relative crystallinity[e]	Crystallite size[f] (nm)
	First	Second	Third							
ZSM-5(250-60,300-30,350-15)	250-60	300-30	350-15	SiO_2	51.2	-	-	-	10.2	52.0
ZSM-5(250-45,300-20,350-10)	250-45	300-20	350-10	SiO_2	110.7	-	-	-	38.5	34.7
ZSM-5(250-30,300-15,350-5)	250-30	300-15	350-5	-	399.0	0.220	0.102	0.118	100	11.6

[a]Total surface areas were obtained by the BET method.

[b]Total pore volumes were estimated from the adsorbed amount at $P/P_0=0.99$

[c]Measured by t-plot method.

[d]$V_{meso}=V_{total}-V_{micro}$

[e]Relative crystallinity: XRD pattern relative intensity at $2\theta=23.2^o$

[f]Crystallite size estimated by Scherre's equation at $2\theta=23.2^o$.

thesis route corresponds to our previous publication [24]. Initially, the appropriate amount of sodium hydroxide was mixed with deionized water at room temperature. Then, sodium aluminate and tetrapropylammonium bromide (TPABr) were added to the mixture and stirred for 1 h. Finally, fumid silica was added gradually to the above solution and aged for 24 h. The resulting gel with composition of $0.0025Al_2O_3 : 1SiO_2 : 0.1Na_2O : 0.1TPABr : 35H_2O$ was obtained. In the next step, the resultant gel was located inside a stainless-steel autoclave, which was heated by different three-step temperature programmed as listed in Table 1. For example, the first sample prepared by three-step temperature programming was denoted as ZSM-5(250-60,300-30,350-15). For treatment, the samples were filtered, washed with deionized water and dried at 110 °C for 12 h. The calcination temperature of 550 °C, which is higher than the maximum temperature needed for decomposition of an organic template (TPA^+ ions) [40], and also calcination time of 15 h were used for the calcination process. This calcination condition was optimized to ensure both the complete elimination of the organic template and the formation of the perfect MFI network. It is in agreement with the literature for the calcination condition for ZSM-5 synthesis [41,42]. So, the dried powders were calcined at 550 °C for 15 h to eliminate the structure-directing agent. Subsequently, the obtained solids were ion-exchanged at 80 °C for 12 h for two times, using 1 M NH_4NO_3 solution, followed by drying at 110 °C and calcination at 500 °C for 4 h.

3. Characterization of Samples

The phase composition and crystalline structure of synthesized materials were characterized by a Bruker D8 Advance diffractometer, which employed CuKα radiation in a scanning range of 2θ= 5-55°. The relative crystallinity was estimated from the intensity of the diffraction peak at 2θ=23.2° used as reference peak and assuming a nominal 100% crystallinity. Applying the Scherrer equation to the broad superlattice peak gives an estimate of the crystallite size. The samples were examined under a scanning electron microscope (FESEM) using HITACHI S-4160 analyzer to study the morphology and particle sizes of zeolites. The X-rays produced from the collision of electrons with the sample were used in energy dispersive analysis (EDX-dot mapping) by a Scan MV 2300 Cam for determining the chemical composition. The specific surface area and pore volumes were obtained by adsorption-desorption of N_2 at 78 K using a Micromeritics ASAP 2020 BET-BJH analysis. Fourier transform infrared spectroscopy (FTIR, UNICAM 4600) was used in the range of 500-4,000 cm^{-1} wave number K-Br pellet method for detecting the surface functional groups. The acid site density and acidic strength of catalysts were determined by TPD/TPR 2900 analyzer. The sample was first degassed at 500 °C under a helium flow rate (50 ml min^{-1}). After the reactor cooled to 50 °C, the sample was saturated with ammonia. For removing the adsorbed ammonia, the sample was then purged with helium flow for about 30 min. Afterward, the sample was heated again at a rate of 10 °C min^{-1} to 800 °C. The thermal conductivity detector (TCD) was used as a function of temperature for measuring the amount of adsorbed ammonia. Finally, thermo-gravimetric analysis (TGA) was performed using a NETZSCH TG 201 F1 machine which was equipped with a mass spectrometer to determine the amount of coke deposition on the deactivated zeolite. The deactivated catalyst was loaded and heated from room temperature to 250 °C in the N_2 flow. Then, the used catalyst was heated to 800 °C in flowing air with a rate of 15 °C/min.

4. Catalytic Performance Test

The catalytic performance test of nanostructured ZSM-5 catalysts in the methanol to propylene reaction was done in the experimental setup [24]. The performance test was carried out in a U-shape fixed bed reactor (i.d.=8 mm, L=32 cm), using 0.4 g of crushed zeolite packed between quartz frits. Before the reaction, the nanostructured ZSM-5 catalysts were preheated with Ar flow at 500 °C for 1 h. The liquid mixture of $CH_3OH : H_2O$ (50 vol% CH_3OH and 50 vol% H_2O) was placed in a saturator with a constant-temperature water bath. Therefore, the vapor pressure of methanol and water was calculated at 15 °C, using the Antoine equation (P_{CH3OH}= 73.9 mmHg and P_{H2O}=13.5 mmHg). According to Raoult's law for an ideal mixture of methanol/water, the concentration of these feeding gases was determined at constant value by Dalton's law (84 vol% CH_3OH and 16 vol% H_2O). Ar stream with a constant flow rate was also used as carrier gas which bubbled through a saturation evaporator and was co-fed into the reactor with gaseous space velocity (GHSV) of 10,500 cm^3/g_{cat}·h. The products were analyzed via a gas chromatograph (GC Chrom, Teif Gostar Faraz, Iran) equipped with a flame ionization detector (FID) and Plot-U capillary column (Agilent). The methanol conversion and products selectivity were calculated as follows:

$$\text{Conversion (\%)} = \frac{(\text{Initial moles of MeOH}) - (\text{Unreacted moles of MeOH})}{(\text{Initial moles of MeOH})} * 100$$

$$\text{Selectivity (\%)} \quad \frac{\text{Mole of specific product in reactor outlet}}{\text{Total moles of whole products}} * 100$$

RESULTS AND DISCUSSIONS

1. Characterizations

1-1. XRD Studies

The XRD patterns of nanostructured ZSM-5(250-60,300-30, 350-15), ZSM-5(250-45,300-20,350-10) and ZSM-5(250-30,300-15,350-5) catalysts are shown in Fig. 1. The formation of the MFI crystal structure during hydrothermal synthesis consists of different stages: aging, nucleation and crystal growth [28]. During the hydrothermal synthesis, a high degree of crystallinity for zeolites can be obtained by complete progress on the hydrothermal stages. Nucleation occurs from supersaturation with the transformation amorphous phase into a crystalline structure. In this stage, the chemical aggregation of species can lead to the formation of different kinds of germ nuclei [30]. Due to crystal growth, the nuclei need to enlarge to a certain size. In this condition, the crystals of the framework start to grow and so result in the appearance of XRD characteristic peaks related to the faces of the crystal. The diffraction peaks exhibit two different types of structures prepared by temperature programmed hydrothermal approach. The peaks at 2θ=8.0, 8.9, 9.1, 14.9, 20.9, 23.2° are characteristic diffraction peaks of tetragonal MFI phase (JCPDS 00-044-0002) [43,44], and the peaks at 2θ=20.9, 26.7, 36.7, 39.6, 42.6, 50.3° are related to

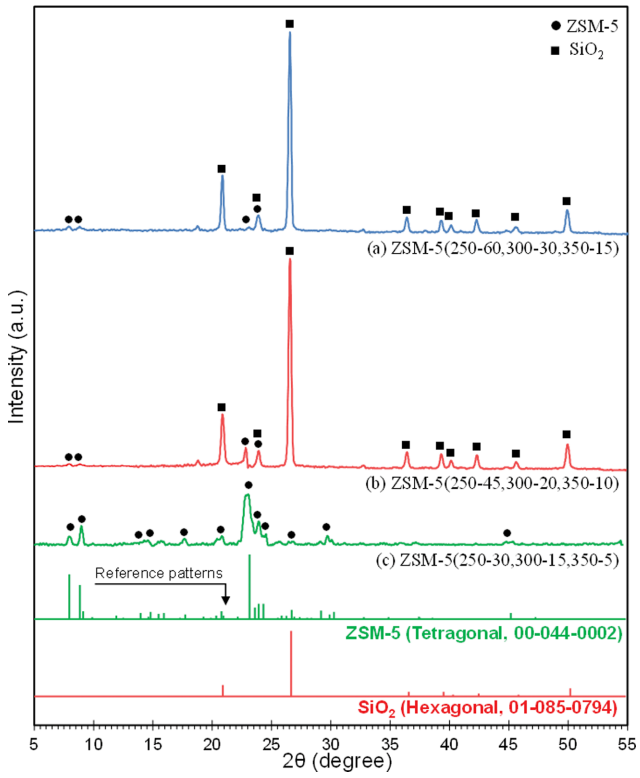


Fig. 1. XRD patterns of nanostructured ZSM-5 catalysts synthesized using three-step high temperature short time method: (a) ZSM-5(250-60,300-30,350-15), (b) ZSM-5(250-45,300-20,350-10) and (c) ZSM-5(250-30,300-15,350-5).

hexagonal SiO_2 particles (JCPDS 01-085-0794) [22,45]. The ZSM-5(250-30,300-15,350-5) sample prepared with short time temperature programmed synthesis has a typical MFI-structure with no impurity phase reported in the literature [8]. Meanwhile, the two other aluminosilicate materials, which were synthesized at longer time temperature programmed, demonstrate the formation of the SiO_2 impurity phase along with the ZSM-5 framework. This is mainly due to the MFI structure transforming to the thermodynamically stable dense oxide phase (SiO_2) occurring during the three-step long time temperature programmed. At shorter crystallization time temperature programmed synthesis, the results are indicated the formation of ZSM-5 phase with low signs of the SiO_2 structure. Moreover, the intensities of peaks differ based on the applied crystallization time. The intensity of the XRD peaks for ZSM-5 molecular sieve synthesized at short crystallization time correlated with the high number of crystal nuclei that appears into the crystalline structure.

The relative crystallinity and crystallite size of the prepared materials are given in Table 1. The relative crystallinity of the MFI products for ZSM-5(250-60,300-30,350-15), ZSM-5(250-45,300-20,350-10) and ZSM-5(250-30,300-15,350-5) catalysts was found to be 10.2%, 38.5% and 100%, respectively. The difference in the crystallinity of the catalysts can be attributed to different crystallization times in varied high temperatures during the three-step hydrothermal synthesis. In addition, dislodgement of Si from the ZSM-5 framework damaged the MFI structure and resulted in a significant decrease in crystallinity of ZSM-5(250-60,300-30,350-15) and ZSM-5(250-45,300-20,350-10) catalysts. Therefore, the ZSM-5(250-30,300-15,350-5) molecular sieve exhibited complete crystallinity with high nucleation density. The average crystallite size of the MFI structure was about 52, 34.7 and 11.6 nm for ZSM-5(250-60,300-30,350-15), ZSM-5(250-45,300-20,350-10) and ZSM-5(250-30,300-15,350-5) catalysts synthesized by three-step hydrothermal condition with different crystallization times. In particular, the results showed that the crystallite size was small at the rapid crystallization of the ZSM-5(250-30,300-15,350-5) catalyst. With increasing the crystallization time at varying high temperatures, the crystallite size of ZSM-5(250-60,300-30,350-15) and ZSM-5(250-45,300-20,350-10) samples significantly increased to 52 and 34.7 nm, respectively. This indicates that a long crystallization time leads to the growth of ZSM-5 crystals at each step of temperature programming and yields larger crystals. However, the three-step high temperature program led to the high rate of nucleation, but the short crystallization time prevented the growth of crystal faces and so led to decreasing the crystallinity. The overall results were an increase in nucleation rate and as well as a decrease of crystal growth to a specific degree, which resulted in small and perfect crystals without amorphous species.

1-2. FESEM Studies

Fig. 2 depicts the FESEM results of the synthesized materials. It is observed that the ZSM-5(250-60,300-30,350-15) and ZSM-5 (250-45,300-20,350-10) catalysts present a similar morphology of SiO_2 particles in the size range of 6-8 μm. There are also some small ZSM-5 grains around the SiO_2 particles. These results can be attributed to the long crystallization time in temperature programmed hydrothermal preparation that allows for the competitive structure production between SiO_2 and ZSM-5 phases. Hence, the agglomeration of dense oxide phase can be observed into ZSM-5 particles in the FESEM images of ZSM-5(250-60,300-30,350-15) and ZSM-5(250-45,300-20,350-10) materials. This is following previous XRD results on the structure of ZSM-5 with different crystallization times. On the other hand, the particles of the ZSM-5 (250-30,300-15,350-5) catalyst have similar coffin morphology in the range of 1-2 μm. This morphology is similar to the reported literature for the shape of ZSM-5 particles [14,17]. Moreover, the formation of smoother particles for the ZSM-5(250-30,300-15, 350-5) catalyst with uniform particle size distribution can be correlated with the proper crystallinity of this sample resulting from the XRD analysis. The resulting crystallization process causes the formation of a high number of crystal nuclei followed by rapid crystallization of the ZSM-5(250-30,300-15,350-5) sample and gradual growth of crystallites, implying the completion of crystal growth and smooth particles with uniform morphology. In particular, the particle sizes of pure ZSM-5 are smaller compared to SiO_2 particles produced as impurity structures. Therefore, it is expected that the ZSM-5(250-30,300-15,350-5) catalyst with small and uniform particles is going to have optimal performance for the conversion of methanol to propylene.

1-3. EDX Studies

Fig. 3 shows the EDX analysis of nanostructured ZSM-5(250-30,300-15,350-5) catalyst. According to EDX data, the existence of Si, Al and O elements indicates the successful formation of aluminosilicate chemical composition into the framework of ZSM-5

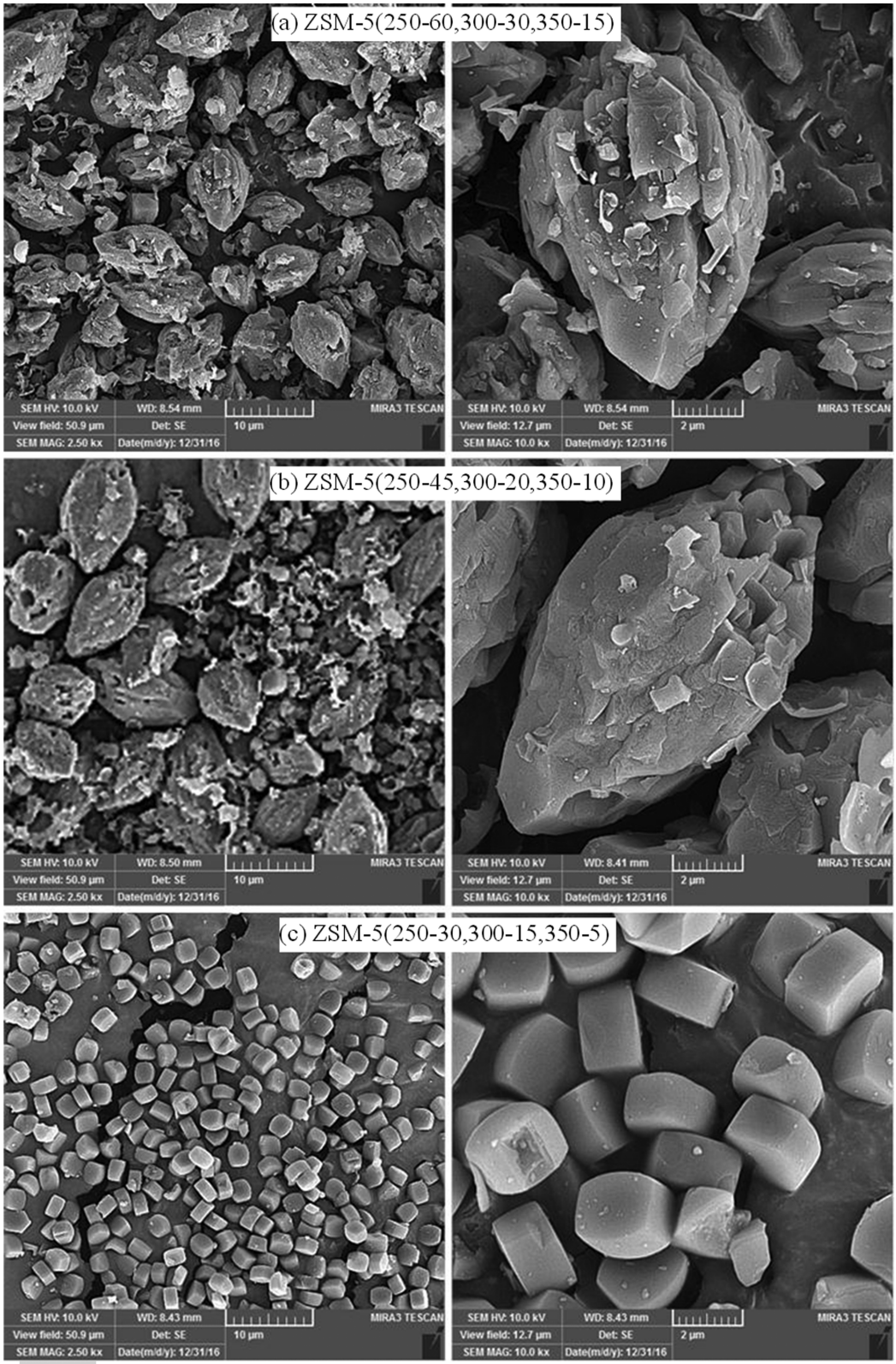


Fig. 2. FESEM images of nanostructured ZSM-5 catalysts synthesized using three-step high temperature short time method: (a) ZSM-5(250-60,300-30,350-15), (b) ZSM-5(250-45,300-20,350-10) and (c) ZSM-5(250-30,300-15,350-5).

(250-30,300-15,350-5) catalyst synthesized by three-step short time temperature programmed. On the other hand, the significant difference in the intensity of Si and Al peaks confirmed the high Si/Al molar ratio (Si/Al=200) in the final ZSM-5(250-30,300-15,350-

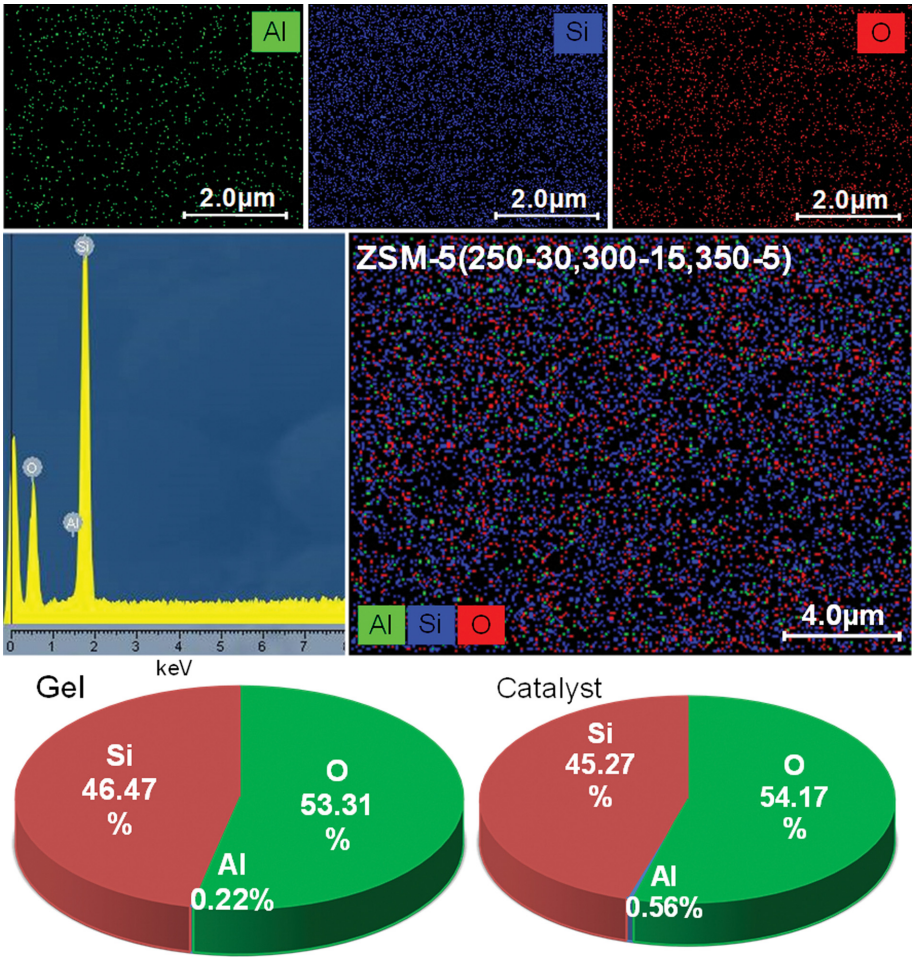


Fig. 3. EDX analysis of nanostructured ZSM-5 catalysts synthesized using three-step high temperature short time method: ZSM-5(250-30,300-15,350-5).

5) product. Therefore, this sample showed a high content of silicon in the ZSM-5 zeolite prepared at short crystallization time and three-step temperature programmed. However, the EDX images indicated the proper distribution of all elements on the surface of the catalyst, which was in good accordance with no amorphous phase observed by FESEM. On the other hand, the silicon atoms exhibited a more homogeneous distribution into the ZSM-5 framework. The appropriate distribution of Si can affect the strength and number of active sites for ZSM-5(250-30,300-15,350-5), causing an increase in the catalytic activity of this sample. According to Fig. 3, the weight percentage of Si, Al and O detected on the surface of the ZSM-5(250-30,300-15,350-5) catalyst was proximately close to those elements used in the gel composition and confirmed that the Si/Al ratio of the ZSM-5(250-30,300-15,350-5) sample was almost the same as the synthesis mixture. This result was also in good agreement with the observations of XRD and FESEM analyses, which confirmed the presence of regular coffin shape materials with no amorphous phase. Furthermore, the low amount of Si in the surface of ZSM-5(250-30,300-15,350-5) nanostructured catalyst can be attributed to the short crystallization time, which prevented complete silica incorporation into the MFI framework. In this regard, Al elements were incorporated on the external surface of crystals and the inner space of the channels. Therefore, a high percentage of Al was exhibited on the surface of the catalyst compared to the gel. On the other hand, the excess O observed on the surface of zeolite demonstrated the formation of different oxygen coordination in the crystalline structure.

1-4. BET-BJH Studies

The N_2 adsorption-desorption isotherms of the ZSM-5(250-30,300-15,350-5) catalyst are presented in Fig. 4. The sample is stored as a type-I isotherm and the hysteresis loop is type-H4, which indicates the microporous feature of ZSM-5(250-30,300-15,350-5) catalyst with some extent of mesopores. These findings are in good agreement with ZSM-5 porous texture as reported in the literature [17,46]. Also, the isotherms have been used to calculate H-K micropore size distributions as shown in Fig. 4. According to the results, the H-K pore size distributions of the ZSM-5(250-30,300-15,350-5) sample are mainly in the range of 4.9-5.5 Å. The results indicate the presence of a different micropore size distribution centered close to each other around 5 Å. Therefore, there are narrow micropore size distributions for ZSM-5(250-30,300-15,350-5) catalyst.

The textural properties of the catalysts are listed in Table 1. The BET specific surface area of ZSM-5(250-60,300-30,350-15), ZSM-5(250-45,300-20,350-10) and ZSM-5(250-30,300-15,350-5) mate-

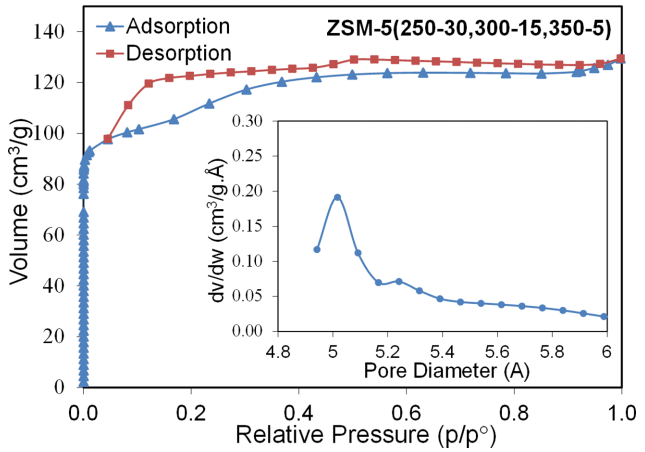


Fig. 4. Adsorption/desorption isotherms and pore size distribution of nanostructured ZSM-5 catalysts synthesized using three-step high temperature short time method: ZSM-5(250-30, 300-15,350-5).

rials are about 51.2, 110.7 and 399.0 m^2/g, respectively. The low specific surface area for ZSM-5(250-60,300-30,350-15) and ZSM-5(250-45,300-20,350-10) catalysts can be attributed to silica existing as impurity species that appeared on the surface of the ZSM-5 particles. Further, the BET result shows the high specific surface area (399.0 m^2/g) for ZSM-5(250-30,300-15,350-5) catalyst, which is in accordance with the small and uniform MFI zeolite particles, as shown by FESEM. The ZSM-5(250-30,300-15,350-5) catalyst also exhibited the total pore volume of 0.220 cm^3/g (V_{micro}: 0.102 cm^3/g and V_{meso}: 0.118 cm^3/g). Therefore, three-step short time temperature programmed hydrothermal synthesis can increase the pore volume without destroying the product framework. These observations are the results of small crystals with higher intercrystalline porosity of the ZSM-5(250-30,300-15,350-5) catalyst.

1-5. FTIR Studies

FTIR spectra of the ZSM-5(250-30,300-15,350-5) sample are given in Fig. 5. Bands occurring in the range of 500-4,000 cm^{-1} indicate the formation of MFI structure in the ZSM-5(250-30,300-15,350-5) catalyst which has a similar trend as reported in the literature [17,42,47]. Therefore, the crystalline ZSM-5 framework can be synthesized by a three-step short time temperature programmed hydrothermal method. The peak in 440 cm^{-1} is related to the characteristic of T-O bending vibration of SiO_4 [8], while the stretching vibration around 540 cm^{-1} is due to five-membered rings as asymmetric stretching [22]. Furthermore, the linkages in SiO_4 or AlO_4 of the ZSM-5 lattices caused bands around 790-1,440 cm^{-1} [48]. The band at 1,710 cm^{-1} is attributed to the physically adsorbed water [24,48]. Also, an additional band was detected in the FTIR results in the region of 3,700 cm^{-1} that corresponded to bridging hydroxyl groups (Si-OH-Al) in the MFI cages [17,22,44]. It is believed that these active sites inside the crystal channels play a major influence on the formation of light olefins during the MTP process.

1-6. TPD-NH_3 Studies

The acidity of a zeolite is an important factor that can refer to acid strength or acid site density. The acid sites of zeolites are significant for catalytic performance; also, understanding the influence of varying acidity strength and acid site numbers can give valuable information on the catalytic behavior during the process. In general, the catalytic activity is affected by the acidic strength and the acid site density. The density of acid sites is the most influential factor for olefin production. Moreover, the level of methanol conversion is affected by the number of acid sites. The low concentration of weak acid sites affects the first step of the reaction path and thereby results in a low interaction of methanol with weak acid sites to produce the DME intermediate species [6,23]. So, the results indicate that the enhanced catalytic activity and progress in olefin production, as the second reaction pathway, are

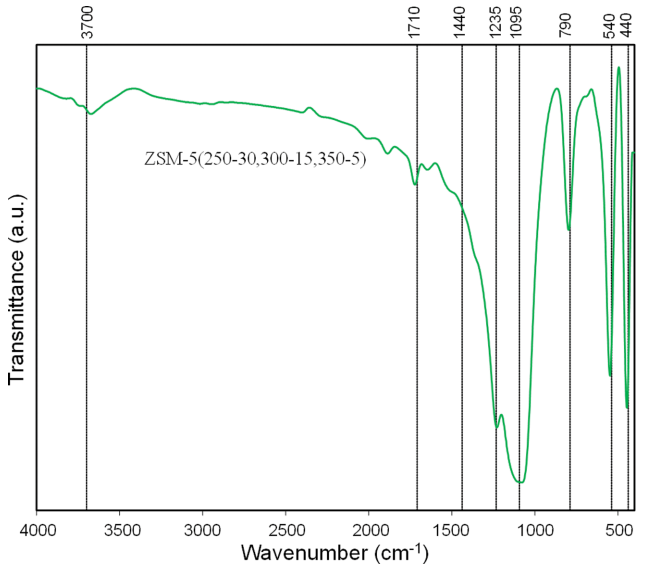


Fig. 5. FTIR spectra of nanostructured ZSM-5 catalysts synthesized using three-step high temperature short time method: ZSM-5(250-30,300-15,350-5).

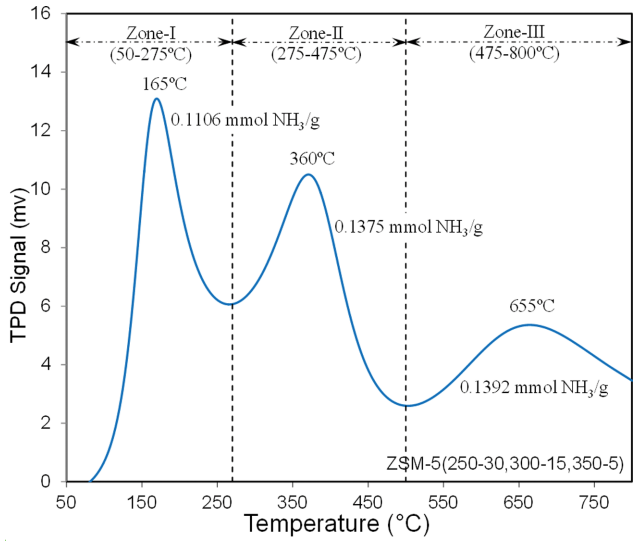


Fig. 6. TPD-NH_3 analysis of nanostructured ZSM-5 catalysts synthesized using three-step high temperature short time method: ZSM-5(250-30,300-15,350-5).

to a significant extent controlled by the weak acid sites of zeolites. On the other hand, the high amount of strong acid sites suppresses the hydrogen transfer reactions and leads to a high rate of coke deposition, while the very low amount of strong acid sites decreases the olefins selectivity due to the covering of active sites by coke deposition [31]. According to the acidic strength, the strong acidity strength can increase the secondary reactions and reduce the lifetime of zeolite during the MTP process. Therefore, proper distribution of acid sites with mild acidic strength can enhance the catalytic properties as well as activity, selectivity and stability [7].

For investigation of catalyst acidity, the TPD-NH_3 results of ZSM-5(250-30,300-15,350-5) zeolite are depicted in Fig. 6. The MFI zeolite was found to have three desorption peaks which were about different strengths of acid sites. On the other hand, the area under these desorption peaks was attributed to the number of acid sites. The peaks occurring in the temperature range of 50-275 °C, 275-475 °C and 475-800 °C for ZSM-5(250-30,300-15,350-5) catalyst were assigned to three kinds of acid sites with weak, moderate and strong acid strength, respectively. The recorded desorption peaks are consistent with reported results for the acidity of ZSM-5 materials [24,49]. The cation concentration and ion exchange capacity decrease by increasing the Si/Al ratio [22,31]. Therefore, the acidity of the ZSM-5(250-30,300-15,350-5) catalyst tends to increase in strength due to the high Si/Al ratio (Si/Al=200). In addition, the different T-atoms can increase the number of possible acid sites for ZSM-5 zeolites. In this regard, TPD measurements revealed that the number of weak acid sites (0.1106 mmol NH_3/g) from the first peak area is lower than the moderate acid site density (0.1375

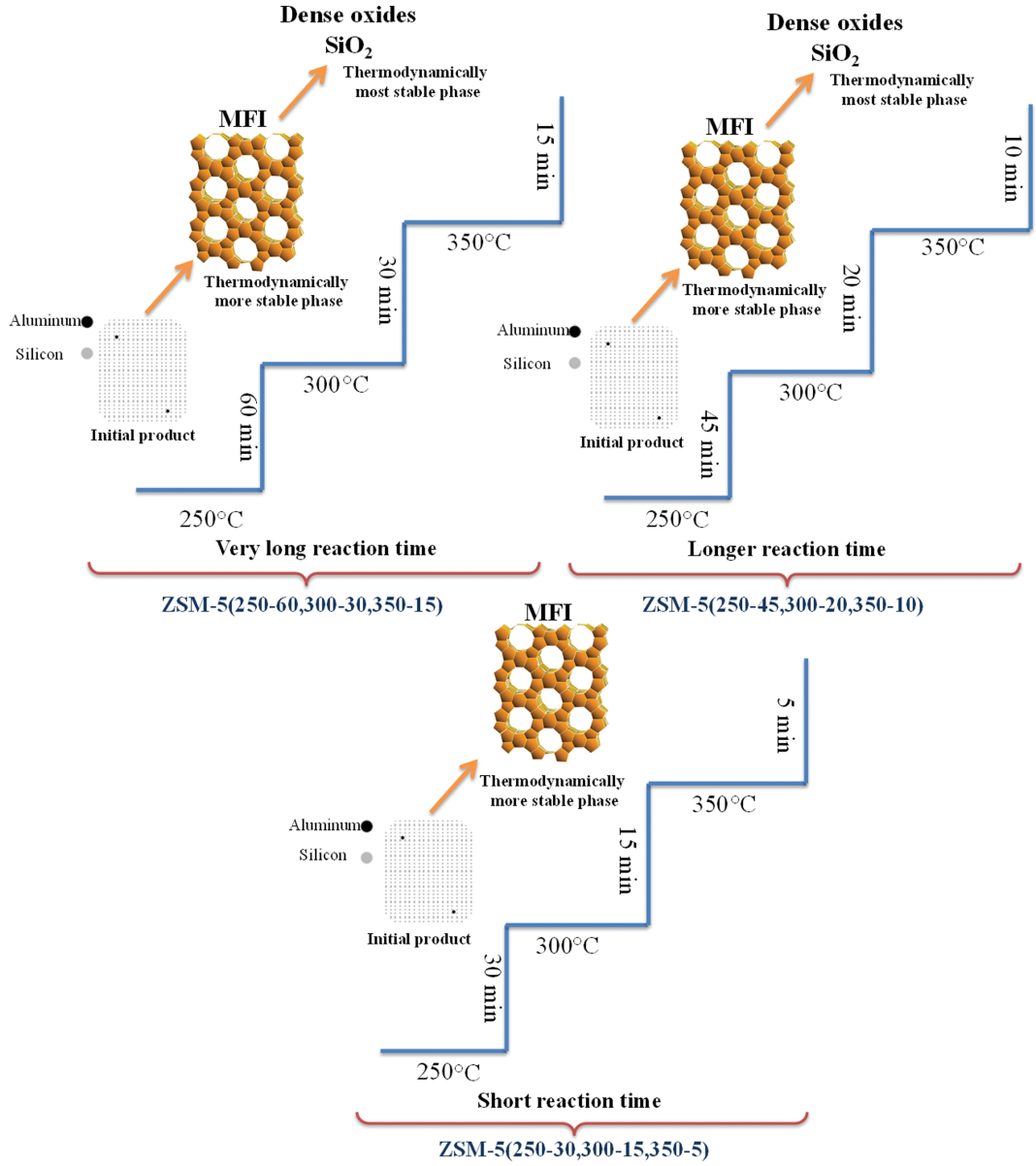


Fig. 7. Reaction pathway for the three-step formation of nanostructured ZSM-5 catalysts synthesized using three-step high temperature short time method.

mmol NH_3/g) and also the concentration of strong acid sites (0.1392 mmol NH_3/g). It is believed that the Al-OH hydroxyl groups cause the formation of weak acid sites, which correspond to the conversion of methanol to DME [7,44]. Therefore, the first step of the reaction pathway for methanol to propylene reaction is progressively favored over weak acid sites of ZSM-5(250-30,300-15, 350-5) zeolite. Moreover, the moderate/strong acid sites have an important role in the formation of C-C bonds with the conversion of intermediate DME products to light olefins [34]. These active sites are the most important type of acidity (Brønsted sites) in the MFI structures generated by the incorporation of Si into the MFI structure. It is found that the high content of Si in the crystalline structure of ZSM-5(250-30,300-15,350-5) relates to a higher concentration of strong/moderate acid sites, and so these observations are favorable to what is observed in the EDX analysis. However, the rates of deactivation are dependent on the number of strong acid sites. But higher acidity can also lead to a lower energy barrier and make the product-forming reactions go faster. This suggests that there is an optimum acidity that has a great influence on the activity of ZSM-5 sample as well as olefin production. Thus, the ZSM-5(250-30,300-15,350-5) catalyst with appropriate distribution of acid sites, plus a higher acidic strength is expected to be an active catalyst in the MTP process.

2. Reaction Pathway of Three-step Synthesis of ZSM-5 at High Temperature

Fig. 7 explains the reaction route for the three-step formation of ZSM-5 zeolites at high temperatures. The temperature and time have important effects on the ZSM-5 catalyst formation, which occurs via a three-step temperature programming at very long reaction times, longer reaction times and short reaction times. In general, the crystallization temperature and duration time of heating were found to be the significant ways for controlling the crystallinity, purity, crystallite size, morphology, pore geometry and acid site distribution of the final product [30,33,36]. The pressure of water as solvent pressure can directly affect the crystallization and framework of catalysts that strongly relate to the crystallization temperature and as well as the duration of the heating [24]. Furthermore, the variation of these parameters may affect the synthesis factors like dissolution, the nucleation process, crystal growth and the phase transition to producing the zeolites with specific pore structures [30].

Among these, the nucleation process and crystal growth have a crucial role in the framework of the synthesized materials. In this regard, the proper temperature should be coupled with optimum crystallization time to obtain the complete chemistry of crystallization and formation of pure crystalline structure. The nucleation and also the linear growth rate can be significantly increased by raising the temperature. Therefore, the crystallinity of the materials is normally improved with time. Also, the morphology of the crystals and as well as the activation energy of the crystal faces can relate to the crystallization temperature. Beyond the proper temperature and time range, the nucleation centers that subsequently grow to create the crystalline structure are disordered under unsuitable crystallization condition [33,34]. Furthermore, the variation in channel dimensions, zeolite pore system and distribution of Si into the zeolite crystalline structure are strongly dependent on the crystallization condition. Therefore, the hydrothermal temperature and time can alter the textural properties and acidity of synthesized materials. By increasing the crystallization temperature and duration for the resultant gel heating, the pore openings and pore volume of zeolites may be decreased, due to the pore blocking with extraframework species formed during this condition [17,24].

The hydrothermal preparation of aluminosilicate materials contains a few elementary stages by which the mixture of Si and Al elements, organic agents and water are converted to a porous crystalline framework by an alkaline supersaturated solution. A typical nucleation mechanism and growth of crystals occur at supersaturation conditions. Therefore, the initial crystalline aluminosilicate products with Si-O-Al linkages are formed for all samples during the first crystallization times. After a certain period, ZSM-5 molecular sieve preparation is governed via an occurrence of efficient phase transformations (Ostwald's law) [24,30]. Phase transformations are attributed to the changes in the stability of the synthesized phase under hydrothermal conditions and can be determined as a competition between two different phases resulting in the production of the thermodynamically most stable phase. For ZSM-5(250-60,300-30,350-15) and ZSM-5(250-45,300-20,350-10) catalysts with long reaction times compared to the ZSM-5(250-30,300-15,350-5) zeolite, the thermodynamically least favorable phase can crystallize first (MFI phase) and then can be replaced by thermodynamically most stable dense oxide SiO_2 structure during the time. The silicate species condensation at this condition at a high temperature can be maximal. Under these conditions, cooperative self-assembly of the silicates may occur. Therefore, the silicate phase condensed further and the formation of the most stable dense oxide SiO_2 increased with increasing hydrothermal time and temperature. So, the reaction time is an effective factor that affects the type of produced phases during the three-step temperature programmed hydrothermal synthesis. Therefore, ZSM-5(250-30,300-15,350-5) catalyst exhibited the pure MFI stable phase synthesized at short crystallization times.

3. Catalytic Performance Studies

3-1. Influence of Catalyst on Methanol Conversion

Fig. 8 shows the methanol conversion over nanostructured ZSM-5(250-60,300-30,350-15), ZSM-5(250-45,300-20,350-10) and ZSM-

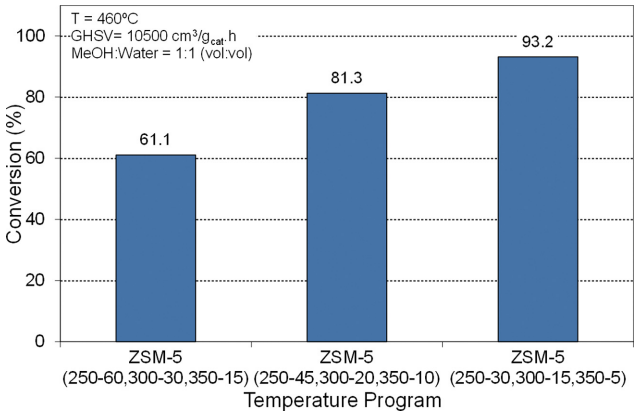


Fig. 8. Methanol conversion over nanostructured ZSM-5 catalysts synthesized using three-step high temperature short time method.

5(250-30,300-15,350-5) catalysts at 460 °C. The conversion of methanol was about 61.1%, 81.3% and 93.2%, respectively. In particular, ZSM-5(250-30,300-15,350-5) catalyst was found to show the highest methanol conversion in comparison with ZSM-5(250-60,300-30,350-15) and ZSM-5(250-45,300-20,350-10) catalysts synthesized at longer crystallization times. The high catalytic conversion of methanol is due to the MFI crystalline framework, specific pore structure and proper acidity distribution of ZSM-5(250-30,300-15,350-5) catalyst. As crystallization time increased, it was found to decrease in methanol conversion for ZSM-5(250-60,300-30,350-15) and ZSM-5(250-45,300-20,350-10) catalysts comparable to that observed in ZSM-5(250-30,300-15,350-5) sample. This is possible since SiO_2 impurities can be detected in the diffraction patterns along with the MFI framework. The impurity species influence the acidity of synthesized materials, thereby decreasing the conversion of methanol. On the other hand, ZSM-5(250-60,300-30,350-15) zeolite showed lower methanol conversion (61.1%) compared to ZSM-5(250-45,300-20,350-10) catalyst (81.3%); this observation along with the physicochemical properties, clearly indicates the large amount of SiO_2 dense phases produced during the long crystallization. As a result, the crystallization rates for any steps of temperature programmed hydrothermal synthesis have a significant effect on the methanol conversion.

3-2. Influence of Catalyst on Products Selectivity

The influence of temperature programmed synthesis on the selectivity of products over nanostructured ZSM-5 zeolites is shown in Fig. 9. Under certain conditions (T=460 °C and GHSV=10,500 cm^3/g_{cat}·h), ZSM-5(250-30,300-15,350-5) catalyst showed the highest selectivity towards ethylene (12%) and propylene (79.5%) compared to ZSM-5(250-45,300-20,350-10) and ZSM-5(250-60,300-30,350-15) zeolites. A remarkably higher olefin selectivity of the ZSM-5(250-30,300-15,350-5) zeolite afforded the low undesired products, which resulted from its physicochemical properties in terms of proper crystallinity, uniform morphology, specific pore structure, and acidity strength. Therefore, the selectivity was very low towards C_4^+ (4%) and also it was negligible towards DME (1%). It can be observed that approximately the same amount of methane was formed for all ZSM-5 nanostructured catalysts. Methane is one of the decomposition materials of the DME produced from cracking and hydrogen transfer reactions [10,12]. For ZSM-5(250-30,300-15,350-5) catalyst, the low selectivity of methane is related to increasingly favorable conditions for olefin production. During long crystallization times, ZSM-5(250-45,300-20,350-10) and ZSM-5(250-60,300-30,350-15) samples produce nearly the same amounts of CH_4 and C_4^+, whereas the ZSM-5(250-60,300-30,350-15) catalyst is more selective to DME than the other zeolite. Therefore, ZSM-5(250-30,300-15,350-5) catalyst has high amounts of light olefins, especially propylene. Also, it can be seen a higher selectivity of DME than C_2-C_3 olefins for both ZSM-5(250-45,300-20,350-10) and ZSM-5(250-60,300-30,350-15) catalysts. This can be ascribed to the extra-framework of Si species from the ZSM-5 framework that decreases the concentration of strong acid sites which are responsible for the production of light olefins from DME. As a result, ZSM-5(250-30,300-15,350-5) catalyst with an improvement in selectivity to light olefins up to 91.5% at nearly complete methanol conversion was used to investigate the influence of time on stream. During the MTP reaction, the small crystallite size of the ZSM-5(250-30,300-15,350-5) sample can compensate for the poor crystallinity of the MFI structure due to affecting the intercrystalline diffusion of molecules and enhancing the catalytic performance. Furthermore, the uniform morphology of particles, proper distribution of acid sites and specific pore geometry for synthesized ZSM-5(250-30,300-15,350-5) zeolite resulted in an active catalyst in the MTP reaction.

3-3. Influence of Time on Methanol to Propylene Reaction

Fig. 10 shows the effect of time on stream performance of ZSM-5(250-30,300-15,350-5) catalyst toward methanol to propylene reaction. ZSM-5(250-30,300-15,350-5) catalyst had maximum methanol conversion (93%) after 200 minutes, while the methanol conversion decreased monotonically and reached 60% after 2,100 minutes on stream. Increasing the reaction time led to the reduction in the availability of active sites by blocking pores and also affected the methanol conversion. In addition, the selectivity towards light olefins (C_2-C_3) was higher than 93% after the first hour. As reaction the proceeded, coke deposition was connected to deactivation and then the selectivity to olefins decreased, reaching a

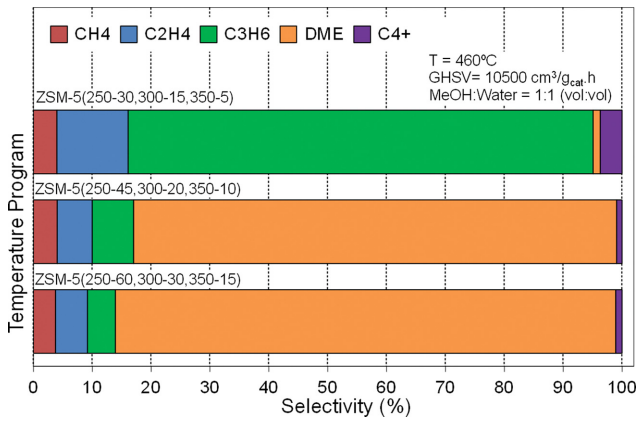


Fig. 9. Effect of temperature program on products selectivities over nanostructured ZSM-5 catalysts synthesized using three-step high temperature short time method.

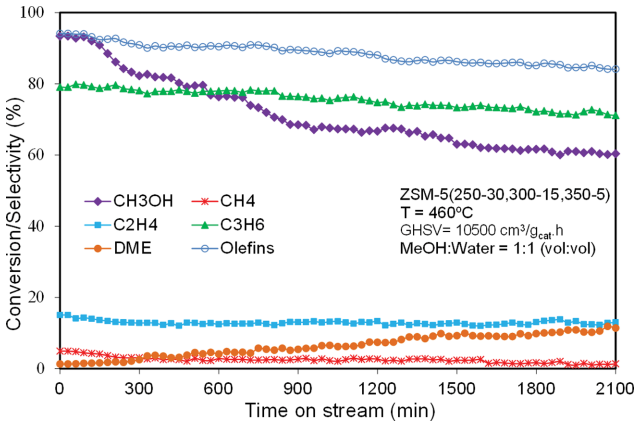


Fig. 10. Time on stream performance of nanostructured ZSM-5 catalysts toward methanol to light olefins: ZSM-5(250-30, 300-15,350-5).

minimum of 84%. However, the selectivity to propylene decreased from 80% to 73% after long time on stream. But, the graph indicates that approximately the same amount of ethylene (11%) was formed regardless of time. On the other hand, lowering the rate of reaction for methane production resulted in less methane formation under the present conditions. In this regard, the existence of strong Brønsted acid sites was favored for light olefins along with hindering undesirable reactions, which caused the reduction of methane selectivity. In general, the reaction path of the methanol to propylene reaction consists of consecutive reaction steps. First, the dehydration of methanol leads to the formation of an equilibrium mixture of methanol, water and DME. The light olefins (C_2-C_3) are then produced from the above mixture in the subsequent step. In the next step, the light olefins are converted to side products via oligomerization and hydrogen transfer reactions. The first step of the reaction path, DME formation from methanol, takes place on the weak acid sites. A methanol molecule reacts with these acid sites to produce a surface methoxy and then undergoes attack by another methanol molecule. Moreover, the moderate/strong acid sites (Brønsted active sites) have an efficient role in the formation of C-C bonds with the conversion of intermediate DME products to light olefins. In this regard, the active sites adsorb certain species as the reaction centers and a surface pool of "-CH_2" is produced via contribution by methanol [40]. By increasing TOS, there was an increase in DME selectivity when the olefins selectivity started to decrease. This observation can be explained by stopping the progress in the second step of the reaction and also the absence of complete DME conversion, due to the reduction in the availability of active sites. Over a long lifetime, the MFI channels were partially blocked by coke deposition and limited access to the acid sites inside the pores. In this regard, the cracking of lighter olefins and hydrogen transfer reactions led to the deposition of coke on the ZSM-5(250-30,300-15,350-5) surface. Therefore, the selectivity towards undesired DME increased substantially with a decrease in the light olefins. Table 2 represents the methanol conversion and propylene selectivity for synthesized ZSM-5(250-30,300-15,350-5) catalyst and typical ZSM-5 samples prepared by the single-step hydrothermal method reported in the literature. As shown, the use of three-step short-time temperature-programmed hydrothermal synthesis instead of the conventional heating method for ZSM-5 preparation led to an enhancement on propylene production, due to the controllable crystallization process which favors the formation of MFI structure with specific textural properties

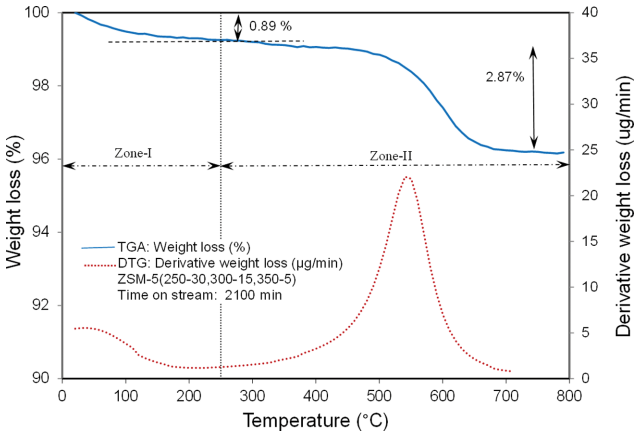


Fig. 11. TGA analysis of nanostructured ZSM-5 catalysts synthesized using three-step high temperature short time method: ZSM-5(250-30,300-15,350-5).

and proper acidity. On the other hand, the multi-step hydrothermal synthesis approach exhibited comparable methanol conversion as the single-step approach but at different reaction times. As a result, compared to the one-step hydrothermal approach, the proposed three-step approach could enhance the catalytic performance of ZSM-5(250-30,300-15,350-5) material compared with those catalysts studied in the literature.

3-4. Deactivation Study

TGA analysis provides important data about the hydrophobicity, dehydration and amount of coke deposition on the used ZSM-5(250-30,300-15,350-5) sample. As shown in Fig. 11, this sample exhibits two distinct steps of weight loss: the first weight loss (25-250 °C) is related to dehydration and the second step (250-800 °C) is related to the coke amount formed during the 2,100 minutes on stream. The low weight loss between 25 and 250 °C is due to the hydrophobic structure of the ZSM-5(250-30,300-15,350-5) catalyst with a high Si/Al ratio. Furthermore, coke formation of the MTP zeolite catalyst is less than 3.0% depending on the lifetime of the ZSM-5(250-30,300-15,350-5) catalyst. This low coking tendency results in excellent catalytic efficiency for ZSM-5(250-30,300-15, 350-5) zeolite employed in the MTP reaction.

CONCLUSIONS

Nanostructured ZSM-5 zeolite was successfully prepared by a

Table 2. Methanol conversion and propylene selectivity of ZSM-5 catalysts synthesized via single-step and multi-step hydrothermal methods

Catalyst	Hydrothermal method		Reaction temperature (°C)	Reaction time (h)	Methanol conversion (%)	Propylene selectivity (%)	Ref.
	Single-step (T°C-Duration h)	Multi-step (T°C-Duration min)					
ZSM-5	150-144	-	370	33	62	65	[22]
ZSM-5	170-48	-	460	40	70	29	[50]
ZSM-5	180-168	-	400	14	58	40	[51]
ZSM-5	190-48	-	400	1.5	98.7	31	[52]
ZSM-5	160-120	-	500	1	100	33.2	[53]
ZSM-5(250-30,300-15,350-5)	-	250-30, 300-15, 350-5	460	35	60	73	This work

three-step short time high temperature programmed hydrothermal method. From the obtained results, it is found that the MFI structure transformed to the more thermodynamically stable SiO_2 phase with prolonging the crystallization times. When the sample was synthesized at 250 °C for 30 min, subsequent 300 °C for 15 min and subsequent 350 °C for 5 min, coffin particles of pure ZSM-5 with uniform particle size distribution were obtained. The low crystallization time for ZSM-5(250-30,300-15,350-5) catalyst could also lead to a high specific surface area (399.0 m^2/g) and proper concentration of strong/moderate active sites. The performance of pure ZSM-5(250-30,300-15,350-5) zeolite synthesized at a short crystallization time was tested in the MTP process. The ZSM-5(250-30, 300-15,350-5) catalyst exhibited the maximum propylene production and also maximum total olefins yield. Therefore, this kind of zeolite prepared at a short time temperature programmed with its proper physicochemical properties would be proposed for the MTP reaction.

ACKNOWLEDGEMENTS

The authors gratefully acknowledge Sahand University of Technology for the financial support of the research as well as Iran Nanotechnology Initiative Council for complementary financial support.

REFERENCES

1. T. Omojola, *Chem. Eng. Sci.*, **251**, 117424 (2022).
2. J. Tuo, J. Lv, S. Fan, H. Li, N. Yang, S. Cheng, X. Gao and T. Zhao, *Fuel*, **308**, 121995 (2022).
3. R. Feng, B. Liu, P. Zhou, X. Yan, X. Hu, M. Zhou and Z. Yan, *Appl. Catal. A: Gen.*, **629**, 118422 (2022).
4. E. Kianfar, S. Hajimirzaee, S. mousavian and A. S. Mehr, *Microchem. J.*, **156**, 104822 (2020).
5. Z. Wan, G. Li, C. Wang, H. Yang and D. Zhang, *Catal. Today*, **314**, 107 (2018).
6. P. Sadeghpour and M. Haghighi, *Particuology*, **19**, 69 (2015).
7. P. Sadeghpour and M. Haghighi, *Asia-Pacific J. Chem. Eng.*, **13**, 2163 (2018).
8. K. Khaledi, M. Haghighi and P. Sadeghpour, *J. Chem. Technol. Biotechnol.*, **95**, 2447 (2020).
9. K. Rahimi, J. Towfighi, M. Sedighi, S. Masoumi and Z. Kooshki, *J. Ind. Eng. Chem.*, **35**, 123 (2016).
10. H. B. Asfha, N. Kang, A. H. Berta, H. Hwang, K. Kim and Y.-K. Park, *Korean J. Chem. Eng.*, **38**, 2047 (2021).
11. A. A. Eslami, M. Haghighi and P. Sadeghpour, *Powder Technol.*, **310**, 187 (2017).
12. H. G. Kim, K. Y. Lee, H.-G. Jang, Y. S. Song and G. Seo, *Korean J. Chem. Eng.*, **27**, 1773 (2010).
13. S. Aghamohammadi, M. Haghighi, P. Sadeghpour and T. Souri, *Comb Chem High Throughput Screen*, **24**, 509 (2021).
14. S. Ahmed, *J. Porous Mater.*, **19**, 111 (2012).
15. Y. Jiao, X. Yang, C. Jiang, C. Tian, Z. Yang and J. Zhang, *J. Catal.*, **332**, 70 (2015).
16. B. Jiang, X. Feng, L. Yan, Y. Jiang, Z. Liao, J. Wang and Y. Yang, *Ind. Eng. Chem. Res.*, **53**, 4623 (2014).
17. P. Sadeghpour, M. Haghighi and A. Ebrahimi, *Ultrason Sonochem*, **72**, 105416 (2021).
18. H.-T. Lee and H.-K. Rhee, *Korean J. Chem. Eng.*, **19**, 574 (2002).
19. T. Zhao, Y. Wang, C. Sun, A. Zhao, C. Wang, X. Zhang, J. Zhao, Z. Wang, J. Lu, S. Wu and W. Liu, *Micropor. Mesopor. Mater.*, **292**, 109731 (2020).
20. M. Li, Y. Huang, C. Ju and Y. Fang, *Micropor. Mesopor. Mater.*, **244**, 7 (2017).
21. F. Meng, Y. Wang, S. Wang, X. Wang and S. Wang, *Comptes Rendus Chimie*, **20**, 385 (2017).
22. B. Mohammadkhani, M. Haghighi and P. Sadeghpour, *RSC Adv.*, **6**, 25460 (2016).
23. A. Izadbakhsh, F. Farhadi, F. Khorasheh, S. Sahebdelfar, M. Asadi and Y. Z. Feng, *Appl. Catal. A: Gen.*, **364**, 48 (2009).
24. P. Sadeghpour and M. Haghighi, *Adv. Powder Technol.*, **29**, 1175 (2018).
25. Y. Zhai, Y. Shang, L. Zhang, X. Meng, Y. Gong, L. Zheng, J. Zhang and P. Liu, *Micropor. Mesopor. Mater.*, **326**, 111374 (2021).
26. K. Chung, K. Kim and G. Seo, *Korean J. Chem. Eng.*, **9**, 144 (1992).
27. Y. Jiao, C. Jiang, Z. Yang, J. Liu and J. Zhang, *Micropor. Mesopor. Mater.*, **181**, 201 (2013).
28. P. Sadeghpour, M. Haghighi and M. Esmaeili, *Comb Chem High Throughput Screen*, **24**, 490 (2021).
29. Z.-Z. Wang, W.-F. Han and H.-Z. Liu, *Catal. Commun.*, **84**, 120 (2016).
30. C. S. Cundy and P. A. Cox, *Micropor. Mesopor. Mater.*, **82**, 1 (2005).
31. A. Amoozegar, M. Haghighi and S. Aghamohammadi, *RSC Adv.*, **6**, 51024 (2016).
32. D. Oleksiak Matthew and D. Rimer Jeffrey, *Rev. Chem. Eng.*, **30**, 1 (2014).
33. M. Dargahi, H. Kazemian, M. Soltanieh, S. Rohani and M. Hosseinpour, *Particuology*, **9**, 452 (2011).
34. E. Aghaei and M. Haghighi, *Powder Technol.*, **269**, 358 (2015).
35. Z. Xu, Y. Wang, J. Zhuang, Y. Li and L. Jia, *Mol. Catal.*, **517**, 111900 (2022).
36. S. S. Mali, P. S. Shinde, C. A. Betty, P. N. Bhosale, W. J. Lee and P. S. Patil, *Prog. Photovoltaics: Res. Appl.*, **22**, 525 (2014).
37. L. Polak, T. P. N. Veeken, J. Houtkamp, M. J. Slaman, S. M. Kars, J. H. Rector and R. J. Wijngaarden, *Thin Solid Films*, **603**, 413 (2016).
38. P. Wang, D. Yang, J. Hu, J. a. Xu and G. Lu, *Catal. Today*, **212**, 62.e1 (2013).
39. W. Wang, L. Li, S. Tan, K. Wu, G. Zhu, Y. Liu, Y. Xu and Y. Yang, *Fuel*, **179**, 1 (2016).
40. F. Yaripour, Z. Shariatinia, S. Sahebdelfar and A. Irandoukht, *Micropor. Mesopor. Mater.*, **203**, 41 (2015).
41. S. Hassanpour, M. Taghizadeh and F. Yaripour, *Ind. Eng. Chem. Res.*, **49**, 4063 (2010).
42. A. Xu, H. Ma, H. Zhang, D. Weiyong and D. Fang, *Polish J. Chem. Technol.*, **15**, 95 (2013).
43. A. Javdani, J. Ahmadpour and F. Yaripour, *Micropor. Mesopor. Mater.*, **284**, 443 (2019).
44. L.-w. Zhang, H.-k. Zhang, Z.-q. Chen, S.-y. Liu and J. Ren, *J. Fuel Chem. Technol.*, **47**, 1468 (2019).
45. Y. Zang, X. Dong and C. Wang, *Chem. Eng. J.*, **313**, 1583 (2017).
46. L. Zeng, F. Liu, T. Zhao and J. Cao, *ACS Omega*, **6**, 19067 (2021).
47. R. Shokrani and M. Haghighi, *Appl. Catal. B: Environ.*, **271**, 118940 (2020).

48. J. Valecillos, E. Epelde, J. Albo, A. T. Aguayo, J. Bilbao and P. Castaño, *Catal. Today*, **348**, 243 (2020).
49. Y. Shang, W. Wang, Y. Zhai, Y. Song, X. Zhao, T. Ma, J. Wei and Y. Gong, *Micropor. Mesopor. Mater.*, **276**, 173 (2019).
50. A. Xu, H. Ma, H. Zhang, W. Ying and D. Fang, *World Acad. Sci., Eng. Technol.*, **7**, 4 (2013).
51. Y. Jin, S. Asaoka, S. Zhang, P. Li and S. Zhao, *Fuel Process. Technol.*, **115**, 34 (2013).
52. H.-J. Chae, Y.-H. Song, K.-E. Jeong, C.-U. Kim and S.-Y. Jeong, *J. Phys. Chem. Solids*, **71**, 600 (2010).
53. N. Hadi, R. Alizadeh and A. Niaei, *J. Ind. Eng. Chem.*, **54**, 82 (2017).